RSC Advances

PAPER

Cite this: *RSC Adv.*, 2015, **5**, 86945

Facile synthesis of a polythiophene/TiO_2 particle composite in aqueous medium and its adsorption performance for Pb(II)†

Jie Chen,[a] Jiangtao Feng*[a] and Wei Yan*[ab]

A polythiophene/TiO_2 (PTh/TiO_2) particle composite was synthesized by a facile and green method *via* $(NH_4)_2S_2O_8$-catalyzed oxidative polymerization of thiophene in acidic aqueous medium to adsorb Pb^{2+} ions from aqueous solution, and the synthesis mechanism was proposed. The particle composite was carefully characterized by Fourier transform infrared spectroscopy (FT-IR), X-ray diffraction (XRD), thermogravimetric (TG) analysis, transmission electron microscopy (TEM), scanning electron microscopy (SEM) and zeta potential analysis, and it showed that the composite prepared had a high specific surface area of 229.66 $m^2\ g^{-1}$. Various factors such as adsorbent dosage and solution pH influencing the adsorption were investigated. The isotherm results indicated that the adsorption performance of Pb^{2+} on the composite fitted the Langmuir model, and the maximum adsorption capacity reached 151.52 mg g^{-1} at 25 °C, 170.36 mg g^{-1} at 35 °C and 173.61 mg g^{-1} at 45 °C. The present adsorption system can be described most favorably by a pseudo-second-order model, confirming that chemisorption such as chelation may be the adsorption rate-limiting step. Meanwhile, adsorption was a spontaneous and endothermic process with increased entropy. In addition, regeneration by HCl-elution and NaOH-activation was possible, and the composite could be used repeatedly without any significant reduction in its adsorption capacity after 6 adsorption–desorption cycles. Furthermore, the adsorption mechanisms were investigated.

Received 23rd July 2015
Accepted 8th October 2015

DOI: 10.1039/c5ra14614c

www.rsc.org/advances

1. Introduction

Lead, which exists extensively in the metal finishing industry, plating plants, battery factories, fertilizer industry, mining operations and military facilities' sewage, is toxic and carcinogenic.[1] Excessive lead ion exposure has been reported to cause kidney, liver, central nervous and reproductive system damage. Lead is also bio-cumulative through food or water, further causing chronic low-grade toxic symptoms such as headaches, irritability, anemia, weakness of muscles and renal damage.[2,3] Much effort has been paid for lead treatment, and the traditional methods including ion-exchange,[4,5] membrane filtration,[6,7] chemical precipitation,[8] solvent extraction,[9] electrochemical treatment,[10] *etc.* have been applied to remove Pb^{2+} from aquatic recipients. However, large scale applications of these methods are difficult to implement due to drawbacks such as large sludge volume generation, high maintenance and operation costs, strict operation conditions, being time consuming, and secondary pollution risks.[2] Compared with these methods, adsorption, which offers the advantages such as low initial cost, easy operation, and insensitivity to toxic substances, appears to be one of the most promising way to remove Pb^{2+} from aqueous solution.[11] A great number of studies have been conducted on lead ion removal by using various low-cost and effective adsorbents, including activated carbons,[12] carbon nanotubes,[13] resins,[14] minerals,[15] bio-adsorbents[16] and agricultural waste materials.[17]

The composites of conjugated polymers and metal oxides have drawn much attention in recent years owning to their perfect properties in electricity, optic and mechanical application.[18–20] TiO_2 is widely applied as a carrier in adsorbent synthesis due to its low cost, good stability, high specific surface area, catalytic and non-toxic nature.[20] Meanwhile, the hydroxyl groups attaching on the surface of TiO_2 can interact with many function groups and metal ions, bringing new prospects for adsorption application and adsorbent modification.[19] Conducting polymers including polyaniline, polypyrrole, polythiophene, *etc.* have attracted considerable attention in many applications. Rathinam Karthik *et al.*[21] described the possibility of using chemically modified chitin with polypyrrole (PPy-*g*-Ch) as an adsorbent for the removal of Pb(II) and Cd(II) ions from aqueous solution. They found that the adsorption capacity of

[a]*Department of Environmental Science and Engineering, Xi'an Jiaotong University, Xi'an 710049, PR China. E-mail: jftes@mail.xjtu.edu.cn; yanwei@mail.xjtu.edu.cn; Fax: +86-29-82664731; Tel: +86-13-032912105*

[b]*State Key Laboratory of Multiphase Flow in Power Engineering, Xi'an Jiaotong University, Xi'an 710049, PR China*

† Electronic supplementary information (ESI) available. See DOI: 10.1039/c5ra14614c

lead onto the PPy-*g*-Ch reached 8.64 mg g^{-1}. Li Yeyun *et al.*[22] successfully synthesized polyaniline modified graphene oxide (PANI/GO) composites by dilute polymerization technique, and the adsorption capacity onto Co(II), Ni(II), Pb(II) and U(VI) ions on PANI/GO composites calculated from Langmuir models were obtained to be 22.28, 25.67, 65.40 and 1552.31 mg g^{-1}, respectively. However, the adsorption capacity for lead onto polypyrrole and polyaniline in the above research is not high enough for practical application. Among these conducting polymers, polythiophene (PTh) has been extensively used in many fields owning to its dramatic optical, semiconducting and electronic characteristics and mechanical properties. Besides, metal ions could be adsorbed by the abundant of sulfur atoms with free lone pairs of electrons in PTh molecule, allowing PTh to be a more excellent adsorbent to uptake metal ions from the wastewater. However, the polymerization of the unsubstituted thiophene was usually carried out in toxic or expensive solvents[23–25] or aqueous medium with the aid of surfactants and complex oxidizing agents due to the low water solubility and an extremely low conversion of thiophene.[26,27] As a result, a new facile and environmental friendly synthetic method of the polythiophene is urgent to be proposed.

In this study, we proposed a facile and environmental friendly synthetic route for the PTh/TiO_2 particle composite by $(NH_4)_2S_2O_8$-catalyzed oxidative polymerization of thiophene in acid aqueous medium, and the composite was carefully characterized. Batch adsorption experiments were carried out to investigate the adsorption performance of PTh/TiO_2 for Pb^{2+} ions. The adsorption isotherm, kinetics, thermodynamics and desorption studies were conducted as well. Furthermore, the adsorption mechanism was proposed according to the results obtained.

2. Materials and experiments

2.1. Materials

Thiophene (98%, Zhejiang Qingquan Pharmaceutical & Chemical Ltd.) was distilled and refrigerated in the dark at 0 °C. HCl (30–33%) and HNO_3 (65–68%) obtained from Beijing Chemical Reagent Co. NaOH, $(NH_4)_2S_2O_8$, citric acid, EDTA-2Na, titanium(IV) isopropoxide (98%) and CH_3COOH purchased from Sinopharm Chemical Reagent Co. Ltd. were of analytical reagent grades. $Pb(NO_3)_2$ (AR) acquired from Tianjin Dengfeng Chemical Reagent Factory was used for the Pb^{2+} solution preparation. The deionized water was gained from an ultrapure water preparation system (EPED-40TF, China).

2.2. Synthesis of the PTh/TiO_2 composite

The typical synthesized process of the composite was in a 500 mL three-jacketed glass reactor with a mechanical stirrer. 0.8 mL of HNO_3 was added in 400 mL of deionized water at 60 °C to prepare the acid solution, and 20 mL of titanium(IV)isopropoxide (0.066 mol) was added in the solution. After being stirred for 60 min, the solution was cooled to room temperature. Then 3.6 mL of thiophene (0.05 mol) was added to the mixture and stirred for 60 min. After that, 20.704 g of $(NH_4)_2S_2O_8$ (0.1 mol) was directly added in, and the mixed solution was stirred for another 24 h at 50 °C. Finally, the powder obtained was filtrated and dried at 50 °C for 24 h. For comparison, TiO_2 was synthesized *via* the same process but without thiophene and $(NH_4)_2S_2O_8$.

2.3. Characteristic analysis

FT-IR spectra were tested by the KBr pellet method on a BRUKER TENSOR 37 FT-IR spectrophotometer in the region between 400 and 4000 cm^{-1}. X-ray diffraction (XRD) patterns of samples were obtained with an X'Pert PRO MRD Diffractometer using Cu Kα radiation. The thermogravimetric (TG) analysis was performed on a Setaram Labsys Evo in N_2 flow and at a heating rate of 10 °C min^{-1}. Transmission electron microscopy (TEM) was performed on a JEM model 2100 electron microscope. The samples were prepared by mixing the sample with ethanol and being ultrasonic vibrated for 1 min, followed by dropcasting 1 to 2 drops of the mixture onto the carbon-coated copper grids and allowed to dry in air. The scanning electron microscopy (JSM-6700F, Japan) was applied to investigate the morphology of sample. Zeta potentials of the composite were obtained *via* a Malvern a Zetasizer Nano ZS90, and the samples were pretreated by adding 5 mg of sample in 10 mL of solutions with various pH values (pH = 1–13, adjusting by 0.1 M HNO_3 or 0.1 M NaOH solution) and being ultrasonic vibrated for 30 min. The BET specific surface area and pore size distribution were determined by a Builder SSA-4200 (Beijing, China) at 77 K. Pore distribution was calculated based on the BJH method using the desorption branch of the N_2 isotherms.

2.4. Influencing factors study

All adsorption experiments were carried out at ambient temperature. The suspension containing adsorbent and 100 mg L^{-1} of Pb^{2+} solution was stirred with speed of 200 rpm for 24 h. Then the suspension was centrifuged at 4000 rpm for 5 min. The concentrations of Pb^{2+} were determined by inductive coupled plasma emission spectrometer (ICPE-9000, Japan).

The influence of adsorbent dosage on the adsorption was carried out by adding various amounts (0.5–3 g L^{-1}) of adsorbent in the Pb^{2+} solution. The effect of pH on adsorption was performed in the Pb^{2+} solutions with different pH values ranging from 1.0 to 6.0. The adsorption capacity q_e (mg g^{-1}) and removal efficiency (%) were calculated according to the equation as follows:

$$q_e = \frac{(C_0 - C_e)V}{m}, \quad (1)$$

$$\text{Removal efficiency} = \frac{C_0 - C_e}{C_0} \times 100\%, \quad (2)$$

where C_0 or C_e (mg L^{-1}) is the concentration of Pb^{2+} in the solution at initial or equilibrium state; m (g) is the mass of adsorbent, and V (L) is the solution volume.

The optimal conditions were employed in the investigations below.

2.5. Batch adsorption and desorption studies

Isotherm experiments were conducted in Pb^{2+} solutions with various initial concentrations ranging from 100 to 1000 mg L^{-1} at 25 °C, 35 °C and 45 °C, respectively. The contact time was 3 h. Kinetics studies were carried out at 25 °C in the Pb^{2+} solution with different initial concentrations (100, 400, 700 mg L^{-1}) in various contact time (0–180 min). 400 mg L^{-1} of Pb^{2+} solution was employed in the thermodynamics procedures for 3 h at different temperature (25, 35, 40, 45 °C). The adsorption amount q_t (mg g^{-1}) was calculated according to the equation as follows:

$$q_t = \frac{(C_0 - C_t)V}{m}, \quad (3)$$

where C_t (mg L^{-1}) is the concentration of Pb^{2+} in the solution at time t (min).

In regeneration investigation, dry adsorbents were added to 20 mL metal ion solution (400 mg L^{-1}) and the mixture was agitated continuously at optimum pH values and equilibrium time to reach its adsorption equilibrium. The adsorbents were withdrawn from the solution, and then 20 mL, 1 mol L^{-1} of HNO_3, HCl, NaOH, citric acid, EDTA-2Na and CH_3COOH were applied separately as elution agents to regenerate the adsorbent for 60 min. The Pb^{2+} concentrations of the supernatants were measured after 5 min centrifugation. The regeneration efficiency (%) was obtained according to the following equations:

$$\text{Regeneration efficiency} = \frac{q_d}{q_a} \times 100\%, \quad (4)$$

where q_d (mg g^{-1}) is the desorbed amount of Pb^{2+} in the elution agent, and q_a (mg g^{-1}) is the adsorbed amount of Pb^{2+} on the PTh/TiO_2 composite.

3. Results and discussion

3.1. Synthesis mechanism of the PTh/TiO_2 composite

The mechanism was proposed for the synthesis of PTh/TiO_2 particle composite in this study (please see Scheme S1†). TiO_2, which may play a role of a micron adsorbent for adsorbing thiophene monomers on its surface or a catalyst, provides a reaction interface or motive promotion for the thiophene polymerization to promote the polymerization process. The polymerization process includes three steps as follows: (a) micron adsorbent (TiO_2) adsorbs thiophene on its surface, (b) the diffusion of $S_2O_8^{2-}$ from bulk to the reaction interface which is full of thiophene, (c) the redox reaction between $S_2O_8^{2-}$ and thiophene to induce the polymerization of thiophene. The acknowledged mechanism for the polymerization of thiophene can be described as follows: the thiophene monomers are oxidized by $(NH_4)_2S_2O_8$ and transformed into their cationic radical forms, followed by combination, deprotonation and polymerization process with the aid of $S_2O_8^{2-}$.[28]

3.2. Characterization of the PTh/TiO_2 particle composite

Fig. 1 shows the FT-IR spectra of TiO_2 and PTh/TiO_2 composite. For comparison, the spectra of thiophene/TiO_2 (Th/TiO_2) were obtained by testing the thiophene added as-prepared TiO_2 (Fig. S1†). From the results, there is little difference between the spectra of Th/TiO_2 and TiO_2 except that the 1491 and 1443 cm^{-1} bands ascribed to C=C symmetric stretching vibrations of the thiophene ring and the peak situated in 774 cm^{-1} ascribed to C–H out-of-plane stretching vibrations are detected in the spectra of Th/TiO_2.[24,29] The possible is that the peaks of thiophene were merged or covered by that of TiO_2. In the spectra of PTh/TiO_2 composite, the absorbances at 659 cm^{-1} suggest C–S in the thiophene ring.[24,29,30] The bands at 1108 and 1047 cm^{-1} belonging to C–H aromatic bending vibrations of the polythiophene[31] may be merged with the bands at 1201, 1134 and 1065 cm^{-1} which attributed to the stretch vibration of SO_4^{2-}, implying the doping of SO_4^{2-} into the PTh/TiO_2 composite.[31] Meanwhile, the peaks ascribed to C=C symmetric and C–H out-of-plane stretching vibrations of the thiophene are also found in the spectra. Besides, adsorption bands at 500–700 cm^{-1} are ascribed to the Ti–O–Ti stretching vibration, indicating the existence of TiO_2.[32] It can be noted that the peak located at 1386 cm^{-1} belonging to stretching vibration of N–O are slightly shifted to 1395 cm^{-1}, and its intensity decreased largely compared to the spectra of TiO_2 and Th/TiO_2, indicating that the TiO_2 may be coated with polymer through the interaction of PTh and $-NO_3$ groups,[33] and the PTh/TiO_2 composite has been obtained.

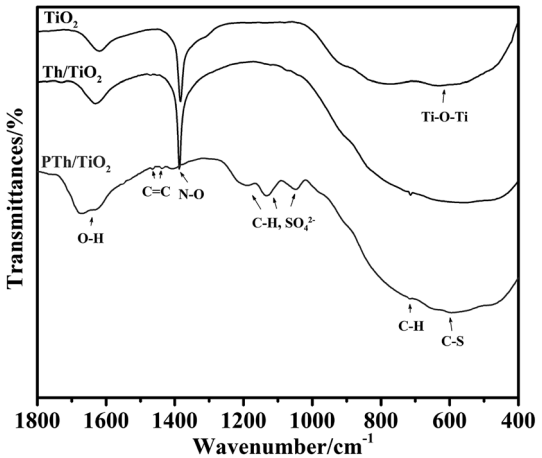

Fig. 1 FT-IR spectra of TiO_2 and PTh/TiO_2 composite.

The XRD patterns of TiO_2 and PTh/TiO_2 composite are illustrated in Fig. 2, and the results show that PTh/TiO_2 composite prepared are purely anatase for the diffraction peaks at 25.3, 37.8 and 48.1 corresponding well to the (101), (004) and (200) planes of anatase TiO_2, respectively,[34] while TiO_2 obtained is a mixture of anatase and rutile. Meanwhile, the peak intensities decease after modification and no new peaks appear in the PTh/TiO_2 pattern, conforming that PTh is all mainly amorphous, and the polymer only covers on the surface of TiO_2 instead of incorporating into the TiO_2 layers.[35]

Fig. 3 shows the TG analysis results of the PTh/TiO_2 composite. The TG curve of the prepared TiO_2 was also investigated. The TG curve of the as-prepared TiO_2 can be divided into two stages. The first stage is from room temperature to 150 °C, over which the mass loss of 6.01% was observed due to the

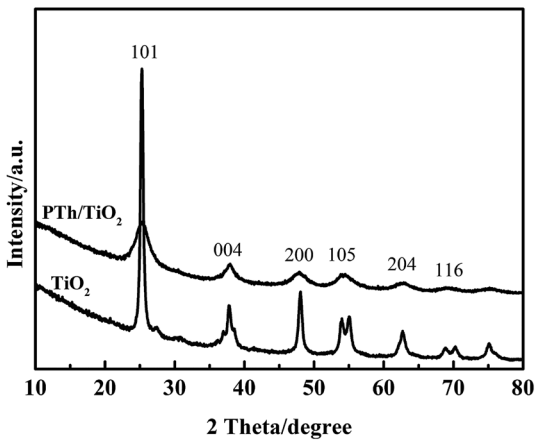

Fig. 2 XRD patterns of the TiO_2 and PTh/TiO_2 composite.

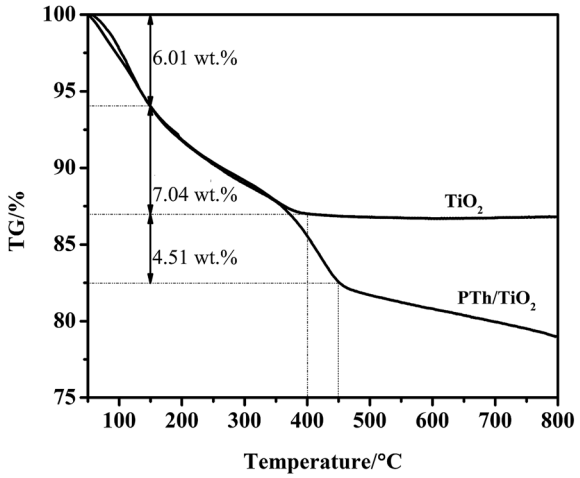

Fig. 3 TG analysis of the prepared TiO_2 and PTh/TiO_2 composite (heating rate of 10 °C min^{-1}, under N_2 gas flow).

adsorbed water on the surface.[36] The second stage is from 150 to 400 °C, where the mass loss is 7.04%. This can be assigned to the strongly bound water or surface hydroxyl groups.[37] Then the mass remains constant from 500 to 800 °C. While the TG curve of the PTh/TiO_2 composite can be divided into three stages. The first step has about 6.01 wt% below 150 °C.[36] The second step between 150 °C and 450 °C is probably assigned to the loss of the strongly bound water or surface hydroxyl groups and the decomposition of PTh.[37] The amount of PTh is approximately calculated to be 4.51 wt% after taking off the amount of the strongly bound water or surface hydroxyl groups. The final weight loss (>450 °C) is possibly ascribed to the decomposition of the sulfated anions chemically adsorbed on the surface of self-prepared TiO_2.[34]

The zeta potentials have great impact on the adsorption capacity of adsorbent for heavy metal ions. According to the literature,[38] some ion exchange occurred on the surface of polymers when the composite is added in a solution, and the composites may be positively or negatively charged according to the following equations:

$$PThX + H^+ \leftrightarrow PThXH^+, (pH < pH_{pzpc}),$$

$$PThX + OH^- \leftrightarrow PThXOH^-, (pH > pH_{pzpc}),$$

where X is the counter anion. As a result, when the solution pH is higher or lower than the pH of zero point charge (pH_{pzpc}), the composite can be negatively or positively charged, leading heavy metal ions to be adsorbed easier or more difficult due to electrostatic force.[38] The zeta potential results of PTh/TiO_2 composite are shown in Fig. 4. It can be seen that the pH_{pzpc} is about 4.17, indicating that the composite is easy to carry negative charges on its surface, and it may more easier to adsorb Pb^{2+} by the electrostatic force.

TEM and SEM were conducted to characterize the as-prepared PTh/TiO_2 composite, and the images were shown in Fig. 5. The analysis shows that the microstructure of the composite is particle, with agglomerated diameter of about 100–200 nm. Meanwhile, the core of the composite with crystal lattice structure covered with amorphous shell is detected in Fig. 5(b), which is consisted with the XRD results, implying successful fabrication of the PTh/TiO_2 nanocomposite.

Textural properties of the composite prepared were evaluated by BET analysis (shown in Fig. S2†). From the N_2 adsorption–desorption isotherms, it can be concluded that there are quantities of micropores existing on the surface of the particle from the fact that the adsorption–desorption isotherms separate slightly.[39] This result is consistent with that of pore size distribution analysis (please see inset of Fig. S2†). The pore size distribution is narrow in the range of 1–5 nm, leading to a high BET surface area of 229.66 m^2 g^{-1}.[40]

3.3. Batch adsorption experiments

3.3.1. Effect of adsorbent dosage. The adsorbent dosage is an important factor influencing the operation cost. The results are depicted in Fig. 6. At the beginning, the removal efficiency increases with the increase of adsorbent amount used due to the more adsorption sites available. However, the adsorption driving force and the adsorbate amount in aqueous solution are

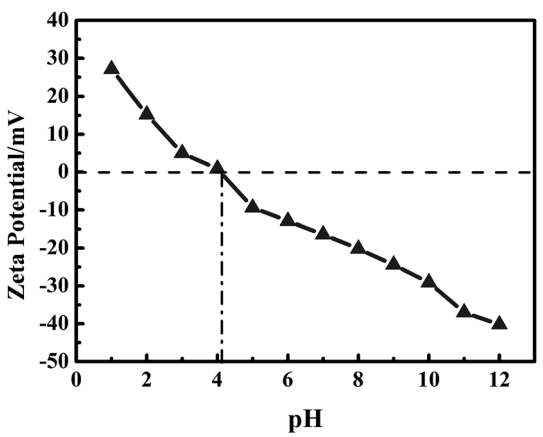

Fig. 4 Zeta potential of the PTh/TiO_2 composite (pH of pretreatment solution, 1–12; dosage, 5 mg; volume, 10 mL; ultrasonic vibrating, 30 min).

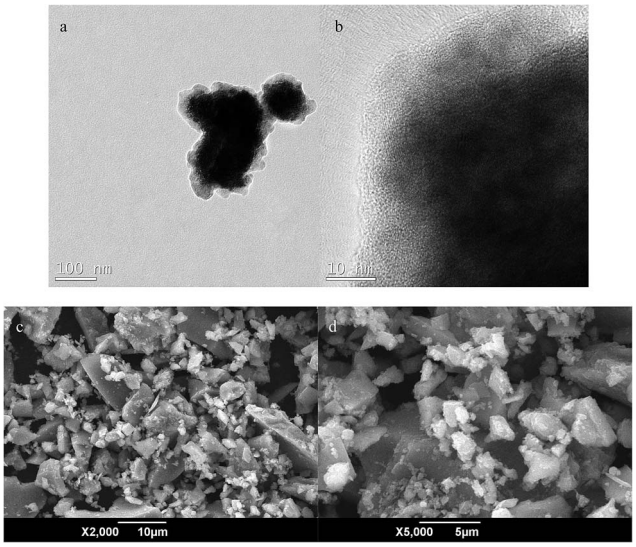

Fig. 5 TEM (a and b) and SEM (c and d) images of the PTh/TiO_2 composite in different scale.

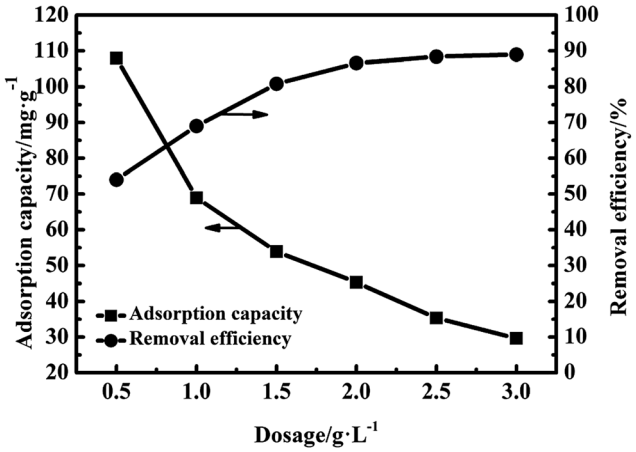

Fig. 6 Effect of adsorbent dosage on the adsorption capacity and removal efficiency of Pb^{2+} onto the PTh/TiO_2 composite (initial concentration, 100 mg L^{-1}; volume, 20 mL; contact time, 24 h; temperature, 25 °C; oscillator speed, 200 rpm; pH value, 6; adsorbent dosage, 0.5, 1.0, 1.5, 2.0, 2.5, 3.0 g L^{-1}).

limited, leading to an adsorption cease if a certain dosage is applied. Meanwhile, the adsorption capacity decreases as dosage increases due to the decrease of surface area.[41] Taking all things into consideration, the 2 g L^{-1} of dosage was chosen, and it was applied in the following studies.

3.3.2. Effect of pH. In this study, effect of solution pH on the adsorption is depicted in Fig. 7. It can be seen that the adsorption capacity and removal efficiency both increased at pH < 3, and changed little at pH > 3. The results indicate that pH plays an important role on adsorption capacity of the as-prepared composite for Pb^{2+}. According to the zeta potential results, when pH value is lower than pH_{pzpc}, the surface of adsorbent is positively charged, while their surface is negatively charged when the pH is larger than pH_{pzpc}.[38] As a result, the

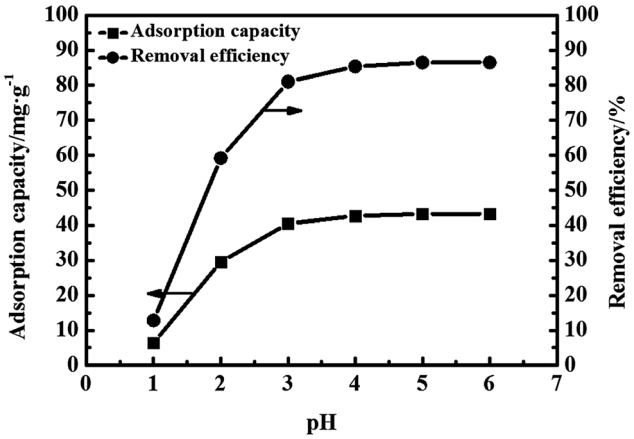

Fig. 7 Effect of solution pH on the adsorption capacity and removal efficiency of the PTh/TiO_2 composite for Pb^{2+} (initial concentration, 100 mg L^{-1}; volume, 20 mL; contact time, 24 h; temperature, 25 °C; oscillator speed, 200 rpm; pH value, 1, 2, 3, 4, 5, 6; adsorbent dosage, 2.0 g L^{-1}).

electrostatic repulsion occurred between the positive charges and Pb^{2+} at pH < pH_{pzpc}. Meanwhile, the pH of the metal ion solution affects the adsorptive process through protonation and deprotonation of functional groups of the ligands in the adsorbent. When the pH of the solution increases, the removal capacity of metal ion is improved due to the lower competition between the protons and metal ions.[15,17] It can be noted that the composite still can adsorb Pb^{2+} at pH < pH_{pzpc} (4.17), indicating that the electrostatic attraction was not the only adsorption mechanism in this system. The optimal pH of 6 was applied in the further experimental studies.

3.3.3. Adsorption isotherm. Adsorption isotherm plays an important role in describing the adsorption capacity and the information about the adsorption sites of adsorbents. Many adsorption models such as the Langmuir,[42] Freundlich,[43] Dubinin–Radushkevich[44] and Temkin[45] models are widely employed to describe the adsorption characteristic between adsorbent and adsorbate (please see ESI†).

The linear forms of four models were used for modeling the adsorption isotherm data. The fitting parameters are listed in Table 1. From the result, the data is fitted better to the Langmuir model (R^2 > 0.990), indicating that the adsorption of Pb^{2+} on the PTh/TiO_2 composite is a monolayer adsorption.[46,47] Meanwhile, the maximum adsorption capacity reaches 151.52 mg g^{-1} (25 °C), 170.36 mg g^{-1} (35 °C) and 173.61 mg g^{-1} (45 °C) from Langmuir model, showing a great promise that the PTh/TiO_2 composite is a good adsorbent for Pb^{2+} removal. The adsorption of Pb^{2+} on the as-prepared TiO_2 was also conducted. The maximum monolayer adsorption capacity reaches 79.63 mg g^{-1} at 25 °C, which was low than that of the composite, indicating a synergetic adsorption and the enhanced adsorption capacity of PTh (please see Table S1†). From the fitting data of Freundlich model, we conclude that the adsorption for Pb^{2+} is favorable due to the small value of $1/n$ ($1/n$ < 1).[48] The free adsorption energies (E) calculated from the Dubinin–Radushkevich model ranges from 8 to 16 kJ mol^{-1}, suggesting that the

Table 1 Adsorption equilibrium parameters acquired from different models in the adsorption of Pb^{2+} onto PTh/TiO_2 composite[a]

	Langmuir model			Freundlich model				D–R model			Temkin model		
	q_m/mg g^{-1}	K_L/L mg^{-1}	R^2	K_F/$L^{1/n}$ $mg^{1/n-1}$ g^{-1}	$1/n$	R^2	K_D/kJ mol^{-1}	q_m/mg g^{-1}	E/J mol^{-1}	R^2	B_T/mg g^{-1}	A_T/L mg^{-1}	R^2
25 °C	151.52	0.0075	0.991	7.80	0.44	0.985	0.0033	132.56	12.31	0.923	44.50	3.38	0.987
35 °C	170.36	0.011	0.995	10.54	0.43	0.957	0.0027	162.97	13.61	0.931	36.85	2.13	0.959
45 °C	173.61	0.025	0.997	26.04	0.30	0.859	0.0025	169.59	14.14	0.989	29.99	0.90	0.990

[a] Condition: initial concentration, 100–1000 mg L^{-1}; volume, 20 mL; contact time, 3 h; oscillator speed, 200 rpm; temperature, 25, 35, 45 °C; pH value, 6; adsorbent dosage, 2.0 g L^{-1}.

adsorption process may be mainly related to ionic exchange or weak chemisorption such as chelation.[49,50] The results obtained from Temkin model show that adsorbates interact with each other during adsorption. The binding energies between adsorbent and adsorbate decrease as temperature increasing, indicating that the adsorption is easier to conduct at higher temperature.[51]

The maximum adsorption capacity q_m obtained from Langmuir model for Pb^{2+} was compared with that of various common adsorbents reported as shown in Table 2. More generally, the adsorption capacity of the PTh/TiO_2 composite for Pb^{2+} is much higher than that of activated carbon (AC), carbon nanotubes, polypyrrole, and polyaniline, and slightly lower than that of commercial exchange resins. In spite of that, the much lower cost and easier synthesis of the PTh/TiO_2 composite in this study make itself more attractive as an adsorbent to remove Pb^{2+}.

3.3.4. Adsorption kinetic. The effect of contact time is shown in Fig. 8. It can be seen that the adsorbed amounts increases sharply in the first 20 min as time and reaches the equilibrium after 60 min. The Pb^{2+} adsorption rate is fast in the first stage owning to the large number of adsorption sites and the high concentration gradient of Pb^{2+}. As the process carries on, the adsorption rate reduces due to the loss of adsorption sites and concentration gradient at the latter stage.[48]

The kinetic of Pb^{2+} adsorption was studied to investigate the adsorption behavior of PTh/TiO_2 composite. The pseudo-first-order model which relates to concentration diffusion, and pseudo-second-order model which determines whether the adsorption process is controlled by chemisorption mechanism, are applied extensively to analyze the kinetic data[60] (please see ESI†).

The fitting parameters for the pseudo-first-order and pseudo-second-order models are listed in Table 3. The experimental results shows that the data is fitted better with the pseudo-second-order model (R^2 > 0.999), confirming that the adsorption process is limited by the chemisorption. However, the chemisorption would be weak according to the results obtained from Dubinin–Radushkevich model, and it may involve valency forces through electron sharing or electron transferring such as chelation between the PTh/TiO_2 composite and Pb^{2+}.[61]

3.3.5. Thermodynamic. The thermodynamic parameters such as Gibbs free energy (ΔG°/kJ mol^{-1}), entropy (ΔS°/J K^{-1} mol^{-1}) and enthalpy (ΔH°/kJ mol^{-1}) obtained from the following equations were applied to determine whether the adsorption process is spontaneous:

Table 2 Adsorption capacity of Pb^{2+} on various common adsorbents

Adsorbents	Adsorption capacity of Pb^{2+} (mg g^{-1})	Ref.
Chemically modified chitin with polypyrrole	8.64	21
AC granular	16.58	12
AC powder	26.94	12
Commercial TiO_2 nanoparticle	21.70	52
AC fibers	30.46	53
Kaolinite	12.10	54
Mesoporous silica	38.02	55
Chitosan–alginate beads	60.27	56
PANI/GO	65.40	22
As-prepared TiO_2	79.63	This work
Activated alumina	83.32	57
Carbon nano tube	118.26	58
PTh/TiO_2	151.52	This work
Lewatit TP 207	198.91	59
Amberlite IRC-718	190.08	14

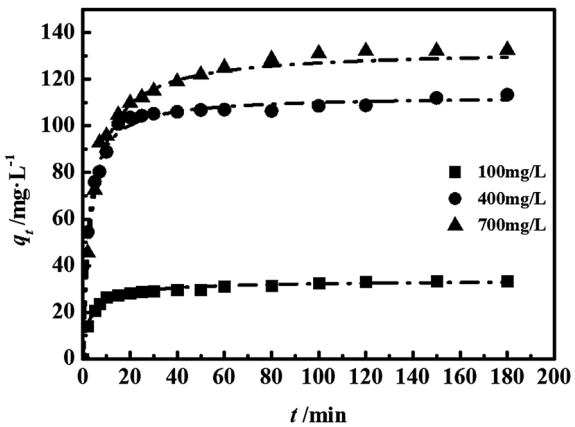

Fig. 8 Contact time *versus* the adsorption behavior of Pb^{2+} onto PTh/TiO_2 composite at various initial concentrations (initial concentration, 100, 400, 700 mg L^{-1}; volume, 20 mL; contact time, 2, 5, 7, 10, 15, 20, 25, 30, 40, 50, 60, 80, 100, 120, 150, 180 min; temperature, 25 °C; oscillator speed, 200 rpm; pH value, 6; adsorbent dosage, 2.0 g L^{-1}).

Table 3 Kinetic parameters of Pb^{2+} adsorption onto the PTh/TiO_2 composite[a]

C_0/mg L^{-1}	The pseudo-first-order model			The pseudo-second-order model			
	k_1/min^{-1}	q_e/mg g^{-1}	R^2	k_2/g (mg min)$^{-1}$	q_e/mg g^{-1}	h/mg (g h)$^{-1}$	R^2
100	0.30	12.92	0.937	44.50	103.84	4665.34	0.999
400	0.018	23.88	0.734	36.85	113.38	7922.98	0.999
700	0.039	75.39	0.981	29.99	137.55	9460.00	0.999

[a] Condition: initial concentration, 100, 400, 700 mg L^{-1}; volume, 20 mL; contact time, 2, 5, 7, 10, 15, 20, 25, 30, 40, 50, 60, 80, 100, 120, 150, 180 min; temperature, 25 °C; oscillator speed, 200 rpm; pH value, 6; adsorbent dosage, 2.0 g L^{-1}.

$$\Delta G^\circ = H^\circ - T\Delta S^\circ, \quad (5)$$

$$\ln K_T = \frac{\Delta S^\circ}{R} - \frac{\Delta H^\circ}{RT}, \quad (6)$$

$$\Delta G^\circ = -RT \ln K_T, \quad (7)$$

where K_T (L mg^{-1}) is the adsorption equilibrium constant equaling $(C_0 - C_e)/C_e$, R (J mol^{-1} K^{-1}) is the gas constant. The fitting results were calculated from the thermodynamics equation and listed in Table 4. The negative values of Gibbs free energy suggest that the adsorption process is spontaneous, and the spontaneity increases with temperature for the ascending number of available adsorption sites and weakening of the boundary layer at higher temperature.[62] The positive value of entropy indicates that the adsorption is a randomness-growth process attributed to the structure changes of adsorbents such as enlargement of pore size during the adsorption. Meanwhile, the adsorption process is endothermic by considering the positive value of the enthalpy, and it might be due to the endothermic diffusion process, deprotonation process and reaction between Pb^{2+} and PTh/TiO_2 composite.[46] The results acquired from thermodynamic showing that heat promotes the adsorption of Pb^{2+} on PTh/TiO_2 composite are consisted with that obtained in the adsorption isotherm and adsorption kinetics investigations.[34]

Table 4 Thermodynamic parameters of Pb^{2+} adsorption onto the PTh/TiO_2 composite[a]

ΔH°/kJ mol^{-1}	ΔS°/J K^{-1} mol^{-1}	Temperature/K	ΔG°/kJ mol^{-1}
0.265	17.08	298	−4.82
		308	−5.00
		313	−5.08
		318	−5.17

[a] Condition: initial concentration, 400 mg L^{-1}; volume, 20 mL; contact time, 3 h; temperature, 25, 35, 40, 45 °C; oscillator speed, 200 rpm; pH value, 6; adsorbent dosage, 2.0 g L^{-1}.

3.3.6. Desorption experiments. In a practical circumstance, excellent regeneration property of an adsorbent is crucial to its application. In this study, 1 mol L^{-1} HNO_3, HCl, NaOH, citric acid, EDTA-2Na and CH_3COOH were applied to extract Pb^{2+} from the composite, and their regeneration and removal efficiency after eluting were also studied (Fig. S3†). It can be found that HCl or HNO_3 have the highest regeneration efficiency but the lowest removal rate while NaOH is the worst elution agent but the best adsorption activator. This result is agreed well with that of pH effect. Based on these facts, 1 mol L^{-1} HCl or HNO_3 was applied as the elution agent and NaOH as the activator afterwards. The adsorption stability of PTh/TiO_2 composite was investigated, as shown in Fig. 9. It revealed that the regeneration efficiency are kept over 90% after regeneration for six times, and the removal rate of Pb^{2+} increase after regeneration for three times dramatically. This may be due to the increase of BET surface area and the enlargement of pore size by treating with the alkali and acid solutions repeatedly. Furthermore, HCl is

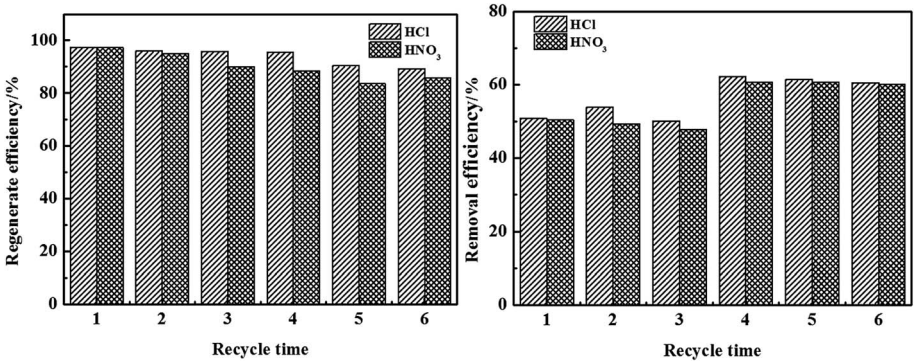

Fig. 9 Adsorption stabilities by HCl/HNO_3-elution and NaOH-activation method of the PTh/TiO_2 composite (initial concentration, 400 mg L^{-1}; volume of Pb^{2+} solution, 20 mL; pH value, 6; adsorbent dosage, 2.0 g L^{-1}; contact time, 3 h; temperature, 25 °C; agitation speed, 200 rpm; recycle time, 6; c(HCl) = 1 mol L^{-1}; c(NaOH) = 1 mol L^{-1}; volume of HCl/NaOH solution, 20 mL).

more suitable to elute the Pb^{2+} ions adsorbed than HNO_3 due to the formation of complex specials such as $PbCl^+$, $PbCl_2$, $PbCl^{3-}$ and $PbCl^{4-}$. Results obtained in this experiment suggest that the as-prepared PTh/TiO_2 composite has stable physical and chemical properties, and can be reused almost without significant decreasing the adsorption capacity.

3.3.7. Adsorption mechanism. FT-IR was applied to investigate the adsorption sites as shown in Fig. 10. It can be seen that the peaks of the O–H, and C–S vibrations shifted from 1597, 659 cm^{-1} to 1502, 635 cm^{-1}, respectively after adsorption. Therefore, we can deduce that Pb^{2+} ions are adsorbed by PTh/TiO_2 composite through interaction of the hydroxyl groups or chelation with S atoms situating in the PTh matrix.[63]

In conclusion, taking the adsorption isotherm and kinetics results into consideration, the adsorption may proceed through the mechanisms as followed. Pb^{2+}, which has unoccupied 5d orbitals, may be adsorbed by chelating with the lone pair electrons of C_π or S atom in PTh through electron pair sharing, and form coordination compounds with a tetrahedral configuration according to the ligand field theory.[64] Besides, the ion exchange between H^+ and Pb^{2+} and electrostatic attraction would be involved by considering the results of pH effect study and desorption experiments.[17] Furthermore, the physical adsorption such as pore adsorption cannot be neglected as well because there are rich pores on the as-prepared PTh/TiO_2 composite. The plausible adsorption mechanism of the PTh/TiO_2 composite for Pb^{2+} was proposed and shown in Scheme 1.

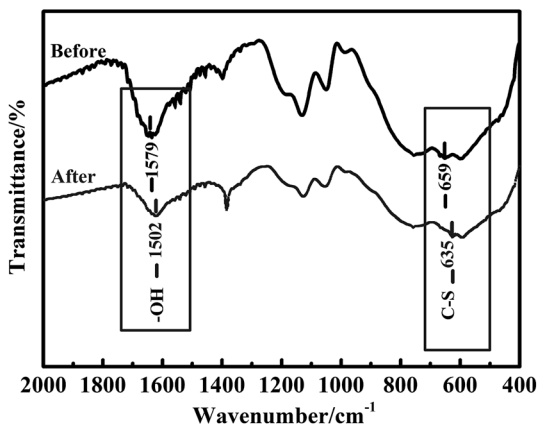

Fig. 10 FT-IR spectra of the PTh/TiO_2 composite before and after adsorption of Pb^{2+} in the region between 400 and 2000 cm^{-1} (KBr pellet method; BRUKER TENSOR 37 FT-IR spectrophotometer).

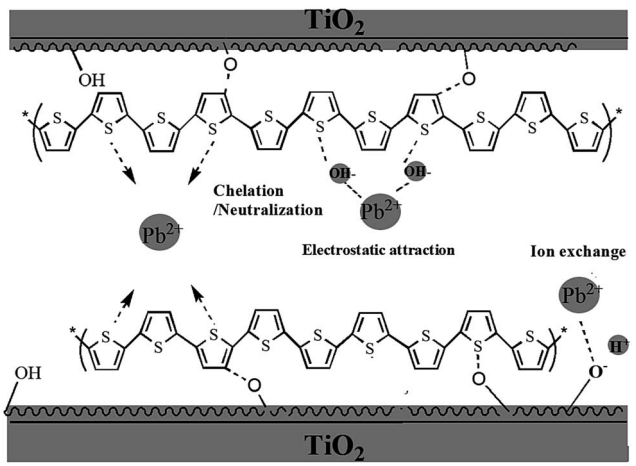

Scheme 1 The possible mechanism for the adsorption of Pb^{2+} onto the as-prepared PTh/TiO_2 composite from aqueous solution.

4. Conclusions

In summary, the PTh/TiO_2 particle composite was successfully synthesized in acid aqueous medium by an environmental-friendly and facile way and carefully characterized. In this process, TiO_2 plays a role of a micron adsorbent for adsorbing thiophene monomers on its surface or catalyst, and provides a reaction interface and motive promotion for the polymerization of thiophene to promote the polymerization process. Its adsorption characteristic for Pb^{2+} was studied with the optimal dosage of 2 g L^{-1} in the solution with optimal pH of 6. The as-prepared PTh/TiO_2 particle composite exhibited a high BET specific surface area reaching 229.66 m^2 g^{-1}. The Pb^{2+} removal efficiency was highly pH dependent, and it increased with pH of Pb^{2+} solution. The adsorption data was fitted well with the Langmuir model, and the maximum adsorption capacities gained from Langmuir model were 151.52 mg g^{-1} at 25 °C, 170.36 mg g^{-1} at 35 °C and 173.61 mg g^{-1} at 45 °C, which were much higher than that of many other commercial adsorbents. Kinetic data were described appropriately by the pseudo-second-order model. The thermodynamic parameters showed that the adsorption is a spontaneous and endothermic process with increased entropy. Results obtained from the desorption experiments proved that the regeneration method by HCl-elution and NaOH-activation was available and the PTh/TiO_2 composite could be used repeat without any significant reduction in its adsorption capacity after 6 adsorption–desorption cycles, suggesting that the PTh/TiO_2 composite was a promising adsorbent for Pb^{2+} removal. Furthermore, the adsorption mechanism investigation suggested that the adsorption of Pb^{2+} onto PTh/TiO_2 composite may mainly through ion exchange and chemisorption such as chelation. Physical adsorption and electrostatic attraction were also involved.

Acknowledgements

The authors gratefully acknowledge the financial supports from the National Natural Science Foundation of China (Grant No. 21307098) and the Specialized Research Fund for the Doctoral Program of Higher Education of China (20090201110005).

References

1 F. Ge, M. M. Li, H. Ye and B. X. Zhao, *J. Hazard. Mater.*, 2012, **211–212**, 366–372.
2 F. Fu and Q. Wang, *J. Environ. Manage.*, 2011, **92**, 407–418.
3 R. Naseem and S. S. Tahir, *Water Res.*, 2001, **35**, 3982–3986.
4 J. B. Diatta, *Pol. J. Environ. Stud.*, 2006, **15**, 219–227.

5 A. Wojtowicz and A. Stoklosa, *Pol. J. Environ. Stud.*, 2002, **11**, 97–101.
6 E. Samper, M. Rodriguez, M. A. de la Rubia and D. Prats, *Sep. Purif. Technol.*, 2009, **65**, 337–342.
7 H. Ozaki, K. Sharma and W. Saktaywin, *Desalination*, 2002, **144**, 287–294.
8 V. C. Taty-Costodes, H. Fauduet, C. Porte and A. Delacroix, *J. Hazard. Mater.*, 2003, **105**, 121–142.
9 C. H. Yun, R. Prasad, A. K. Guha and K. K. Sirkar, *Ind. Eng. Chem. Res.*, 1993, **32**, 1186–1195.
10 M. Belkacem, M. Khodir and S. Abdelkrim, *Desalination*, 2008, **228**, 245–254.
11 K. G. Bhattacharyya and S. Sen Gupta, *Adv. Colloid Interface Sci.*, 2008, **140**, 114–131.
12 H. K. An, B. Y. Park and D. S. Kim, *Water Res.*, 2001, **35**, 3551–3556.
13 H. J. Wang, A. L. Zhou, F. Peng, H. Yu and J. Yang, *J. Colloid Interface Sci.*, 2007, **316**, 277–283.
14 T. Vaughan, C. W. Seo and W. E. Marshall, *Bioresour. Technol.*, 2001, **78**, 133–139.
15 J. Peric, M. Trgo and N. Vukojevic Medvidovic, *Water Res.*, 2004, **38**, 1893–1899.
16 R. S. Juang and H. J. Shao, *Water Res.*, 2002, **36**, 2999–3008.
17 Z. Reddad, C. Gerente, Y. Andres and P. le Cloirec, *Environ. Sci. Technol.*, 2002, **36**, 2067–2073.
18 K. Bourikas, M. Stylidi, D. I. Kondarides and X. E. Verykios, *Langmuir*, 2005, **21**, 9222–9230.
19 S. Asuha, X. G. Zhou and S. Zhao, *J. Hazard. Mater.*, 2010, **181**, 204–210.
20 M. Janus, E. Kusiak, J. Choina, J. Ziebro and A. W. Morawski, *Desalination*, 2009, **249**, 359–363.
21 R. Karthik and S. Meenakshi, *Int. J. Biol. Macromol.*, 2015, **78**, 157–164.
22 Y. Li, Z. Liu, J. Yang, C. Li, J. Li, Y. Jiang and Y. Dong, *Korean Chem. Eng. Res.*, 2014, **52**, 781–788.
23 S. K. Kang, J.-H. Kim, J. An, E. K. Lee, J. Cha, G. Lim, Y. S. Park and D. J. Chung, *Polym. J.*, 2004, **36**, 937–942.
24 A. Gok, M. Omastova and A. G. Yavuz, *Synth. Met.*, 2007, **157**, 23–29.
25 Y. Zhu, S. Xu, L. Jiang, K. Pan and Y. Dan, *React. Funct. Polym.*, 2008, **68**, 1492–1498.
26 S. S. Jeon, S. J. Yang, K.-J. Lee and S. S. Im, *Polymer*, 2010, **51**, 4069–4076.
27 Z. Zhang, F. Wang, F. e. Chen and G. Shi, *Mater. Lett.*, 2006, **60**, 1039–1042.
28 J. Roncali, *Chem. Rev.*, 1992, **92**, 27.
29 M. R. Karim, C. J. Lee and M. S. Lee, *J. Polym. Sci., Part A: Polym. Chem.*, 2006, **44**, 5283–5290.
30 A. Gök, M. Omastová and A. G. Yavuz, *Synth. Met.*, 2007, **157**, 23–29.
31 X. F. Ma, G. Li, H. Z. Xu, M. Wang and H. Z. Chen, *Thin Solid Films*, 2006, **515**, 2700–2704.
32 X. Y. Li, D. S. Wang, G. X. Cheng, Q. Z. Luo, J. An and Y. H. Wang, *Appl. Catal., B*, 2008, **81**, 267–273.
33 X. Zhang and R. B. Bai, *J. Mater. Chem.*, 2002, **12**, 2733–2739.
34 J. Li, Q. Zhang, J. Feng and W. Yan, *Chem. Eng. J.*, 2013, **225**, 766–775.
35 X. Jin, M. Jiang, J. Du and Z. Chen, *J. Ind. Eng. Chem.*, 2014, **20**, 3025–3032.
36 J. Xu, P. Yao, X. Li and F. He, *Mater. Sci. Eng., B*, 2008, **151**, 210–219.
37 K. Nagaveni, G. Sivalingam, M. S. Hedge and G. Madras, *Appl. Catal., B*, 2004, **48**, 83–93.
38 X. Zhang and R. B. Bai, *Langmuir*, 2003, **19**, 10703–10709.
39 Y. Junjie, W. Decheng and Y. Zhenglong, *J. Phys. Chem. C*, 2008, **112**, 17156–17160.
40 C. Zhang, J. Sui, J. Li, Y. Tang and W. Cai, *Chem. Eng. J.*, 2012, **210**, 45–52.
41 Y. S. Ho, *Water Res.*, 2006, **40**, 119–125.
42 I. Langmuir, *J. Am. Chem. Soc.*, 1918, **40**, 1361–1403.
43 H. Freundlich, *Z. Phys. Chem., Stoechiom. Verwandtschaftsl.*, 1906, **57**, 385–470.
44 M. M. Dubinin, E. D. Zaverina and L. V. Radushkevich, *Zh. Fiz. Khim.*, 1947, **21**, 1351–1362.
45 M. Temkin and V. Pyzhev, *Acta Physicochim. URSS*, 1940, **12**, 327–356.
46 T.-t. Li, Y.-g. Liu, Q.-q. Peng, X.-j. Hu, T. Liao, H. Wang and M. Lu, *Chem. Eng. J.*, 2013, **214**, 189–197.
47 A. H. Chen, C. Y. Yang, C. Y. Chen, C. Y. Chen and C. W. Chen, *J. Hazard. Mater.*, 2009, **163**, 1068–1075.
48 D. L. Zhao, G. D. Sheng, J. Hu, C. L. Chen and X. K. Wang, *Chem. Eng. J.*, 2011, **171**, 167–174.
49 I. Mobasherpour, E. Salahi and M. Pazouki, *J. Saudi Chem. Soc.*, 2011, **15**, 105–112.
50 M. Islam, P. C. Mishra and R. Patel, *Chem. Eng. J.*, 2011, **166**, 978–985.
51 M. L. Zhang, H. Y. Zhang, D. Xu, L. Han, D. X. Niu, B. H. Tian, J. A. Zhang, L. Y. Zhang and W. S. Wu, *Desalination*, 2011, **271**, 111–121.
52 S. Mahdavi, M. Jalali and A. Afkhami, *Chem. Eng. Commun.*, 2013, **200**, 448–470.
53 K. Kadirvelu, C. Faur-Brasquet and P. le Cloirec, *Langmuir*, 2000, **16**, 8404–8409.
54 S. Sen Gupta and K. G. Bhattacharyya, *J. Environ. Manage.*, 2008, **87**, 46–58.
55 Y. Liu, Z. C. Liu, J. Gao, J. D. Dai, J. A. Han, Y. Wang, J. M. Xie and Y. S. Yan, *J. Hazard. Mater.*, 2011, **186**, 197–205.
56 W. S. W. Ngah and S. Fatinathan, *J. Environ. Sci.*, 2010, **22**, 338–346.
57 T. K. Naiya, A. K. Bhattacharya and S. K. Das, *J. Colloid Interface Sci.*, 2009, **333**, 14–26.
58 M. A. Tofighy and T. Mohammadi, *J. Hazard. Mater.*, 2011, **185**, 140–147.
59 P. Brown, I. A. Jefcoat, D. Parrish, S. Gill and E. Graham, *Adv. Environ. Res.*, 2000, **4**, 19–29.
60 A. R. Kul and H. Koyuncu, *J. Hazard. Mater.*, 2010, **179**, 332–339.
61 C. Septhum, S. Rattanaphani, J. B. Bremner and V. Rattanaphani, *J. Hazard. Mater.*, 2007, **148**, 185–191.
62 A. M. El-Toni, M. A. Habila, M. A. Ibrahim, J. P. Labis and Z. A. Alothman, *Chem. Eng. J.*, 2014, **251**, 441–451.
63 R. B. Shubo Deng and J. Paul Chen, *Langmuir*, 2003, **19**, 5058–5064.
64 J. Zhu, J. Yang and B. Deng, *Environ. Chem. Lett.*, 2009, **8**, 277–282.